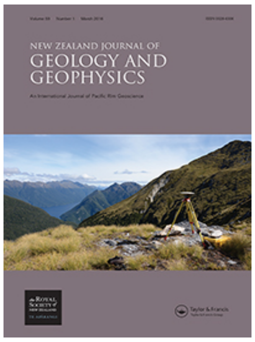

Taylor & Francis
Taylor & Francis Group

New Zealand Journal of Geology and Geophysics

ISSN: 0028-8306 (Print) 1175-8791 (Online) Journal homepage: https://www.tandfonline.com/loi/tnzg20

New Zealand GPS velocity field: 1995–2013

John Beavan, Laura M Wallace, Neville Palmer, Paul Denys, Susan Ellis, Nico Fournier, Sigrun Hreinsdottir, Christopher Pearson & Mike Denham

NEW ZEALAND JOURNAL OF GEOLOGY AND GEOPHYSICS, 2016
VOL. 59, NO. 1, 5–14
http://dx.doi.org/10.1080/00288306.2015.1112817

Taylor & Francis
Taylor & Francis Group

RESEARCH ARTICLE

New Zealand GPS velocity field: 1995–2013

John Beavan[a†], Laura M Wallace[b], Neville Palmer[a], Paul Denys[c], Susan Ellis[a], Nico Fournier[a], Sigrun Hreinsdottir[a], Christopher Pearson[c] and Mike Denham[c]

[a]GNS Science, Lower Hutt, New Zealand; [b]Institute for Geophysics, Univerity of Texas, Austin, TX, USA; [c]School of Surveying, University of Otago, Dunedin, New Zealand

ABSTRACT
We collate nearly two decades of campaign GPS data gathered at over 900 sites throughout New Zealand to release a New Zealand nationwide GPS velocity field. The data span the entire North and South islands of New Zealand with a typical spacing of 10–20 km and a denser network (c. 2–8 km spacing) in the Wellington region, central Taupo Volcanic Zone and parts of the Arthur's Pass area. The dataset provides the most comprehensive-to-date view of crustal deformation within the Australia–Pacific plate boundary zone in the New Zealand region. We discuss the data acquisition, processing and derivation of the velocities and uncertainties. We also undertake corrections for earthquake displacements to obtain a velocity field that is largely representative of interseismic deformation between 1995 and 2013.

ARTICLE HISTORY
Received 2 June 2015
Accepted 1 October 2015

KEYWORDS
Deformation; geodesy; global positioning system; neotectonics; New Zealand

Introduction

The New Zealand plate boundary zone has long fascinated geoscientists, partly due to the diversity of active tectonic processes that are represented there from subduction (and intra-arc rifting) in the North Island at the Hikurangi subduction zone, to strike-slip on the Marlborough Fault Zone, transpressional collision along Alpine Fault and finally back to subduction again at the Puysegur Trench offshore Fiordland. Over the last two decades, Global Positioning System (GPS) methods have served as an important method to obtain a detailed picture of the distribution of contemporary crustal deformation throughout New Zealand's diverse plate boundary zone.

GPS methods have been widely used since the early 1990s to track crustal deformation at plate boundaries. Continuously operating GPS (cGPS) sites offer the best way to capture time-varying tectonic processes; they are expensive however, and require infrastructure that in many cases make installation of dense cGPS networks prohibitive. Alternatively, campaign GPS datasets (which are obtained by periodic measurements at permanent survey marks) provide an economically viable means of establishing a spatially denser network, although lacking the temporal resolution of cGPS. Campaign GPS surveys are an important method of obtaining a time-averaged snapshot of the deformation rates within a plate boundary zone at a high spatial resolution. This is particularly so in areas where logistics, environmental conditions and/or cost prohibit dense installation of cGPS sites. Campaign GPS measurements have revolutionised our view of the distribution and kinematics of deformation at plate boundary zones (Beavan & Haines 2001; Wallace et al. 2004, 2007; Zhang et al. 2004; Reilinger et al. 2006; McCaffrey et al. 2007; Shen et al. 2011; Elliott et al. 2013), and have also refined our understanding of seismic hazard in these regions (e.g. Mazzotti et al. 2011; Stirling et al. 2012).

An extensive campaign GPS dataset has been acquired throughout New Zealand since the early 1990s. Here, we present velocities derived from 18 years' worth of data, gathered at over 900 sites during GPS campaigns between 1995 and 2013 (Figure 1). The network is densest in the Wellington region, central Taupo Volcanic Zone and parts of the Arthur's Pass region (c. 2–8 km spacing between GPS sites), and is sparsest in the less tectonically active Northland region of the North Island (>50 km spacing). In the remainder of the country, campaign GPS sites are generally spaced at 10–20 km. This represents one of the densest, most comprehensive campaign GPS datasets ever collected at a major, large-scale (e.g. >1000 km) plate boundary zone, and is rivalled only by datasets that have been gathered at large-scale plate boundaries in the western United States and Japan. We note that comparable datasets spanning similarly large-scale plate boundary zones are typically gathered by many different research groups who are often working independently of each other, focusing on small portions of the plate boundary. In contrast, it is important to note that most of the New Zealand dataset has been acquired under the leadership of the late John Beavan. This collaborative effort has resulted in uniform,

CONTACT LM Wallace lwallace@utexas.edu
†John Beavan (1950–2012)
Supplementary material available online at www.tandfonline.com/10.1080/00288306.2015.1112817

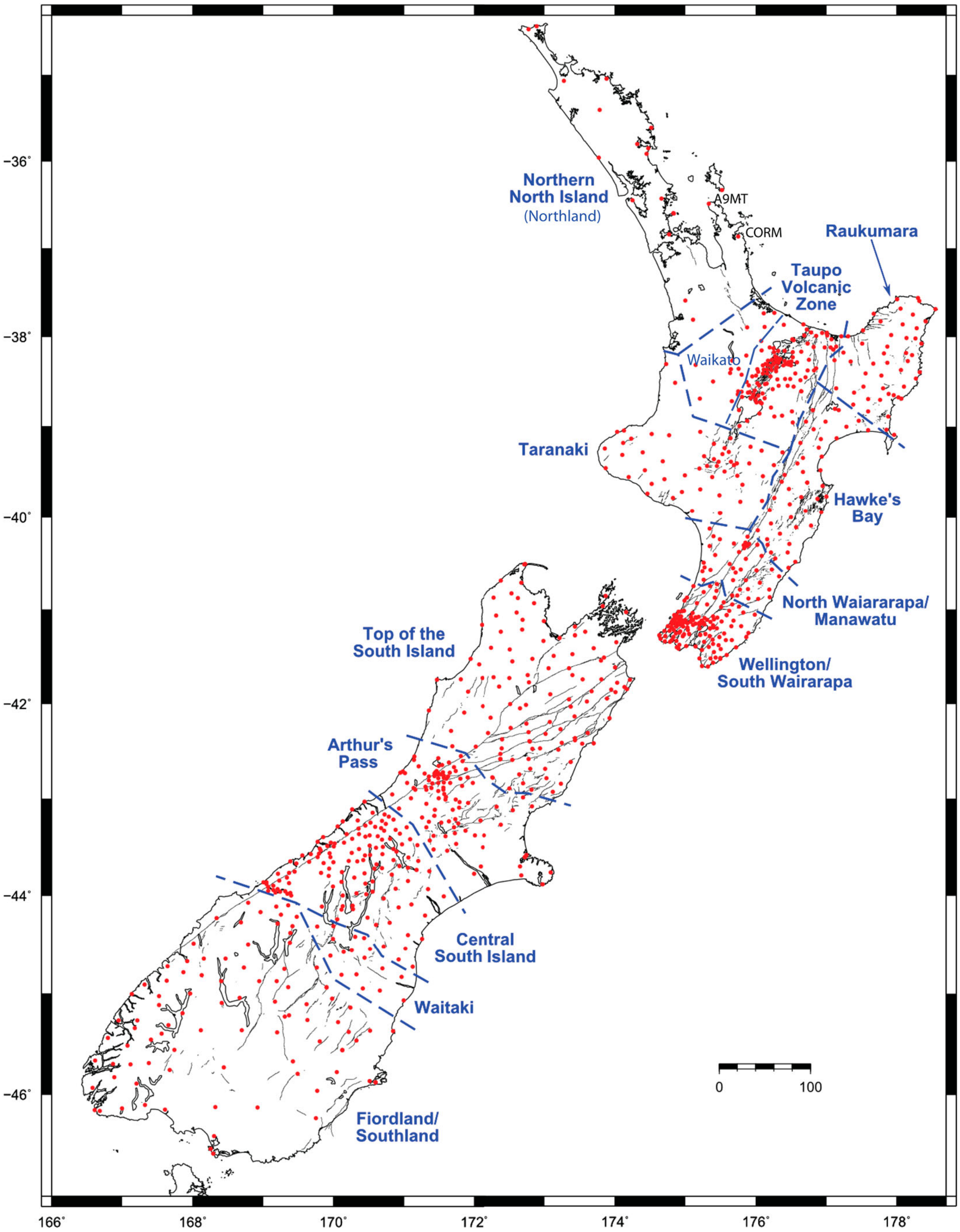

Figure 1. Map of campaign sites with campaign region outlines.

comprehensive, national coverage of crustal deformation data throughout the New Zealand plate boundary, making the existence of this dataset all the more remarkable. Here, we present the details of the GPS data acquisition and processing along with the velocity field data.

The New Zealand campaign GPS dataset

The GPS velocity field presented here is derived from numerous GPS campaigns conducted throughout New Zealand. GPS campaign data acquisition in New Zealand began in the early 1990s, largely through the efforts of Desmond Darby and Graeme Blick, formerly of the New Zealand Department of Science and Industrial Research (now GNS Science), with important assistance from Chuck Meertens at UNAVCO in the United States. John Beavan arrived in New Zealand in the mid-1990s and was instrumental in ramping up the scale of campaign GPS measurements in New Zealand. Under John's leadership, the campaign network continued to grow and expand. The resulting network now comprises over 900 stations distributed throughout the country (Figure 1).

Since 2002, GPS campaigns have been conducted in New Zealand typically once per year, taking place in the summer months in a different region of New Zealand, alternating between the North and South islands each year (Figure 1). We have divided New Zealand into eight different regions to define the footprint of each campaign, with the entire country being re-measured approximately every 8 years (Table 1). Prior to 2002, more frequent and regionally extensive campaigns were undertaken to establish a base of measurements throughout the country, resulting in coverage of much of the country during this period. Some of the mid-1990s measurements in the South Island were augmented by campaigns undertaken by Oxford University in collaboration with GNS Science and Richard Walcott at Victoria University of Wellington. In the last 10 years, various one-off funding opportunities from the New Zealand Earthquake Commission and other sources have also enabled more frequent re-measurement of networks in the Taupo Volcanic Zone and the southern North Island. Many of the sites in central Otago have also seen more frequent measurements (not included in this table). The School of Surveying at the University of Otago has installed the Central Otago Deformation network (COD; Denys et al. 2014), consisting of 33 marks. Initially in 2004 the COD network comprised five marks that were observed every 3 months; as the number of marks increased, the measurement frequency decreased to 6-month campaigns (2007–2011) and annual campaigns (2012–2013). The New Zealand dataset has also benefited from occasional nationwide campaigns (1997, 1998, 2006) to observe all first-order survey marks, which is a national network of survey marks that help to connect the 1949 New Zealand Geodetic Datum (NZGD49) to the 2000 New Zealand Geodetic Datum (NZGD2000). The Fiordland and Christchurch regions have also seen more frequent campaign observations to document deformation following large earthquake sequences (Reyners et al. 2003; Petersen et al. 2009; Beavan et al. 2010, 2011a, 2011b, 2012). Table 1 details the years in which the various campaigns were undertaken.

The velocity field we derive in this paper is based on data gathered between 1995 and 2013, and is similar to that used most recently by Wallace et al. (2012a). Most of the velocities have been updated however, benefiting from the addition of more recent (2009–2013) campaign data from various parts of New Zealand. These data have been used in numerous papers to define the overall kinematics and rates of crustal deformation throughout the New Zealand plate boundary zone (e.g. Darby & Meertens 1995; Bourne et al. 1998; Beavan et al. 1999, 2007, 2010, 2011a, 2011b, 2012; Darby et al. 2000; Beavan & Haines 2001; Darby & Beavan 2001; Moore et al. 2002; Nicol & Beavan 2003; Wallace et al. 2004, 2007, 2012a; Ellis et al. 2006a, 2006b; Nicol & Wallace 2007; Holden et al. 2015; among many others).

In each campaign GPS sites are observed for at least two sessions with session lengths of 18–24 hours, but as short as 7–8 hours in a very few cases (most of these shorter sessions were during the mid-1990s campaigns). A variety of receiver types have been used for the fieldwork including Ashtech Z-XII and μZ, Trimble 4000 (SSE and SSi), 5700, R7 and NetRS receivers. Most of the GPS campaign data were acquired using either choke ring antennas (Trimble and Ashtech), Trimble L1/L2 compact antennas with ground plane or Trimble Zephyr Geodetic antennas. For the last 10 years, the vast majority of the campaign measurements have been undertaken with Trimble 5700 and R7 receivers and Zephyr Geodetic Antennas, which helps to minimise any problems arising from antenna mixing. We note that Zephyr Geodetic antennas are also being used by GeoNet, New Zealand's continuous GPS network (www.geonet.org.nz). Many of the campaign GPS benchmarks in New Zealand consist of a survey pin installed in a mostly buried concrete block that is well-connected to the ground. When possible, some sites are installed in bedrock, constructed by securing the survey pin into rock with epoxy. Many of the campaign measurements are performed using a tripod and a rotating optical plummet to set up over the survey mark. Many of the campaign sites are existing survey marks that are also used by local surveyors, which often have a survey beacon on them that we either: (a) mount the antenna on top of; or (b) temporarily remove the beacon to enable set up over the mark with a tripod. Most of the sites in the Central Otago Deformation network are 5/8" threaded rod installed directly in bedrock, using a short adaptor for the antenna during each occupation.

GPS data processing

The GPS carrier phase data from all surveys were processed by methods similar to those described in Wallace et al. (2004, 2012a), using Bernese software version 5.0 (Dach et al. 2007) to determine daily estimates of relative coordinates and their covariance matrices. In addition to the campaign GPS data, we also include in the processing c. 20 of the longer-running continuous GPS sites in Land Information New Zealand's PositioNZ network (http://apps.linz.govt.nz/positionz/index.aspx) and the GeoNet network (http://www.geonet.org.nz), and several IGS stations in the southwest Pacific region on the Australian and Pacific plates. Of more than 9500 station-days of data, about 3% of station observations are rejected at the Bernese processing stage because they appear as outliers (residuals greater than three standard errors) in single-survey variation of coordinate solutions. Some poorly determined station observations are rejected as a result of observing sessions being too short. We account for ocean loading using Topex 7.1

Table 1. Years of campaigns.

Year	Campaign region
1995	Raukumara, Hawke's Bay, TVZ (Rotorua area), Central South Island, Otago/Southland, southern North Island, Waikato (western part of TVZ region), northern North Island
1996	South Island west coast, TOPS
1997	Arthur's Pass, partial TOPS, Raukumara and Hawke's Bay, NZFO, some Wellington sites
1998	Central South Island, Waitaki, Wairarapa, NZFO, some Arthur's Pass, some TVZ
1999	TOPS, Wellington/Wairarapa, some TVZ sites, Canterbury
2000	Arthur's Pass, TVZ (Rotorua area), Taranaki
2001	Raukumara, Fiordland/Southland, Hawke's Bay, Waitaki
2002	Central South Island, Arthur's Pass, Wellington/Wairarapa
2003	Taranaki, Fiordland (select sites)
2004	TOPS, Fiordland (select sites), subset of Raukumara and Wellington
2005	Fiordland (select sites), TVZ
2006	Fiordland/Southland, Arthur's Pass, NZFO
2007	Wellington/Wairarapa, TVZ, Fiordland (selected sites)
2008	Arthur's Pass
2009	Raukumara, Hawkes Bay, selected TVZ, selected Fiordland, Wellington
2010	Central South Island, Fiordland (selected), Canterbury
2011	Taranaki and TVZ, Canterbury
2012	TOPS
2013	Wellington/Wairarapa, Canterbury, Northern North Island

NZFO, New Zealand First Order Network; TOPS, Top of the South Island; TVZ, Taupo Volcanic Zone.

ocean load tides (e.g. FES2004) from Onsala Space Observatory (http://holt.oso.chalmers.se/loading/). We use orbits and polar motion files in the IGS08 reference frame from the IGS, with the associated absolute antenna phase centre files for both satellite and receiver antennas. IGS final orbits and earth orientation parameters are held fixed. Tropospheric delays are estimated hourly, using dry Niell (1996) mapping functions. Ambiguities are fixed using Bernese's quasi-ionosphere-free strategy and the global ionosphere

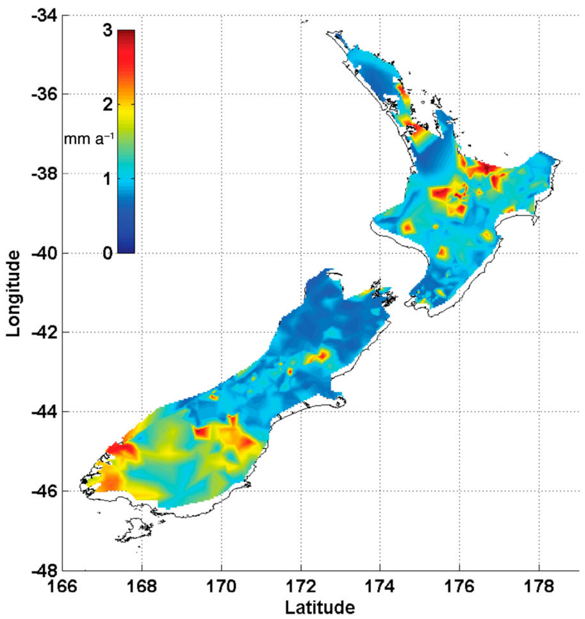

Figure 2. Spatial distribution of velocity uncertainties in the New Zealand velocity field, in terms of $(\sigma_e^2 + \sigma_n^2)^{1/2}$, where σ_e is east uncertainties and σ_n is north uncertainties, in mm a^{-1} (east and north uncertainties from Table S1).

model produced by the Center for Orbit Determination in Europe (CODE).

Obtaining a velocity field in ITRF 2008 and Australian Plate fixed frames

To obtain velocities from daily processing of the GPS sites in a well-defined terrestrial reference frame, we combine SINEX files from the Bernese daily solutions (see previous section) with MIT's daily global solutions of the IGS network using GLOBK (Herring et al. 2010). With GLOBK we estimate a rotation and translation of each daily solution into the ITRF2008 reference frame (e.g. Altamimi et al. 2012). To accomplish this, we tightly constrain the coordinates of a subset of the most reliable core IGS GPS stations to their known ITRF2008 values. We calculate the velocities and uncertainties at each GPS station by a linear fit to the daily ITRF2008 coordinate time series (see the next section for details on how we addressed outliers and coseismic/postseismic deformation prior to velocity calculations; Table S1).

Formal uncertainties of GPS velocity estimates are known to be unrealistically small (e.g. Zhang et al. 1997; Williams et al. 2004). We use the approach of Zhang et al. (1997) to incorporate random walk noise σ_{RWN} and σ_{WN} white noise into the velocity uncertainties at each site, defined

$$\sigma_{\mathrm{RWN}} = \frac{A_{\mathrm{RWN}}}{\sqrt{T}}$$

and

$$\sigma_{\mathrm{WN}} = 2\sqrt{3}\,\frac{A_{\mathrm{WN}}}{\sqrt{N}\,T}$$

where A_{RWN} is the amplitude of random walk noise, A_{WN} is the amplitude of white noise, T is the duration of the time series, and N is the number of data observation points. Since we are dealing with campaign GPS data, it is not possible to determine the amplitude of random walk noise and white noise from the data time series themselves. Beavan (2005) analysed 2–5 years of data from several New Zealand continuous GPS sites, and obtained estimates for white noise and random walk noise amplitudes. We use the Beavan (2005) white noise values (1.1 mm a^{-1} for east and north components) in our campaign velocity uncertainty estimation. However, random walk can be difficult to estimate with short time series (Langbein 2012), and we expect that the random walk noise from Beavan (2005) is likely too large (c. 2 mm a$^{-1/2}$) due to the short duration of NZ cGPS sites available at the time. Here, we assume a random walk noise amplitude of 1 mm a$^{-1/2}$, similar to the mean random walk estimated by Dmitrieva et al. (2015) from a network of long-running cGPS sites in North America; 1 mm a$^{-1/2}$ is also the preferred value used in an analysis of campaign and continuous GPS sites in southern California (Shen et al. 2011). In Figure 2, we provide a summary of how the uncertainties vary spatially in New Zealand by plotting a map view of $(\sigma_e^2+\sigma_n^2)^{1/2}$ (where σ_e is east uncertainties and σ_n north uncertainties). The uncertainties are largest in the southern half of the South Island, due in part to the our removal of all of the post-2009 campaign data in the southern portion of the South Island because of effects from the 2009 M_w 7.8 Dusky Sound earthquake (see discussion in 'Outlier removal and coseismic deformation' below). The large uncertainties in Fiordland (southwestern South Island) are also a consequence of the disruption of the time series by earthquakes in 2003, 2007 and 2009. Most other areas of large uncertainties are related to a combination of fewer observations and/or a shorter duration of campaign measurements (see Table S1).

Rather than viewing the velocities in a reference frame such as ITRF2008, it is more instructive for crustal deformation purposes to view the New Zealand velocity field in a plate-fixed reference frame such as an Australian or Pacific Plate fixed frame. We solve for a pole of rotation for Australia relative to ITRF08 using the velocities we obtain for sites on the Australian Plate (ALIC, CEDU, DARW, HOB2, KARR, NOUM, TID2, TIDB, TOW2, YAR2). Our best-fitting ITRF08/Australia pole of rotation is located at 32.34° N, 37.66°E, with a rotation rate of 0.635° Ma^{-1}. The misfit of Australian plate site velocities to this best-fitting ITRF08/Australia pole is generally less than 0.3 mm a^{-1} (see Table S1). We then rotate the ITRF2008 velocity field for New Zealand into an Australian Plate fixed frame using this pole of rotation (Figure 3). In addition to the velocities of the New Zealand campaign (and some continuous) sites, we also include the velocities of these Australian Plate sites in Table S1. Figure 4 shows the New Zealand velocities relative to the Pacific Plate using the ITRF2008/Pacific pole of DeMets et al. (2014; Pacific Plate relative to ITRF08: 62.544°S, 110.817°E, 0.68° Ma^{-1}). We expect that their ITRF2008/Pacific pole is the most reliable one to use, as they use a larger number of sites on the Pacific Plate than our study or other previous studies.

Outlier removal and coseismic deformation

Following the GLOBK stage, the time series for each site is visually inspected for outliers using the time series viewing tool, TSview (Herring & McClusky, http://www-gpsg.mit.edu/~tah/GGMatlab/). These outliers were removed before the final velocity estimation. We also removed 56 velocities (of 995) from the dataset that were clearly incompatible with the rest of the GPS velocity field. Most of these removed velocities are from sites that have only been observed on two campaigns, over a short span of time (<2 years) or at sites where it was not possible to reliably address coseismic displacements in nearby earthquakes.

Several large earthquakes have impacted the New Zealand campaign GPS network during the period 1995–2013, particularly in the South Island of New Zealand (Table 2). To avoid coseismic and postseismic deformation from the 2010–2011 sequence of earthquakes near Christchurch (Beavan et al. 2010, 2011a, 2012; Gledhill et al. 2011), we have simply removed from our velocity calculations all campaign data collected after the Darfield 2010 M_w 7.1 earthquake at sites that experienced significant (>5 mm) displacement during the 2010/2011 earthquake sequence (Beavan et al. 2010, 2011a, 2012). Generally, this included sites within c. 100 km of the earthquake sequence. Dealing with the effects from earthquakes that have occurred in the Fiordland region since 2003 is much more complicated as the 2003 Secretary Island, 2007 George Sound and 2009 Dusky Sound earthquakes have all impacted parts of the southern South Island. There were insufficient data collected at most GPS sites in Fiordland prior to the 2003 Secretary Island earthquake to enable robust determination of interseismic velocities using only the pre-2003 data. To remove the effect of the Dusky 2009 M_w 7.8 earthquake and subsequent postseismic deformation from this event, which has impacted GPS sites across much of the southern half of the South Island (Beavan et al. 2011b), we removed all campaign data from after July 2009 in the southern half of the South Island from our velocity determination. The August 2003 Secretary Island and October 2007 George Sound earthquakes were more complicated to deal with, since they occurred in the middle of the time series. For sites impacted by the M_w 7.1 Secretary Island event, we removed all data between the earthquake and the end of 2004 (to avoid any influence from coseismic slip and poseismic afterslip), and calculated an offset in the time series during the earthquake using TSview. Only the pre-2003 earthquake and post-2004 data (corrected for the earthquake offset) are therefore used in the velocity determination. We implemented a similar approach to correct for the M_w 6.7 George Sound earthquake. However, due to the uncertainties in removing the Secretary Island and George Sound earthquake displacements from the campaign GPS time series, we advise caution in the use and interpretation of the GPS velocities from the Fiordland region.

We also note that the 23 December 2004 M_w 8.1 Macquarie Island earthquake produced noticeable displacements at continuous GPS sites in New Zealand. Southernmost South Island sites were displaced by up to 10 mm, decreasing to <5 mm in the central South Island and to <1–2 mm in the North Island (Watson

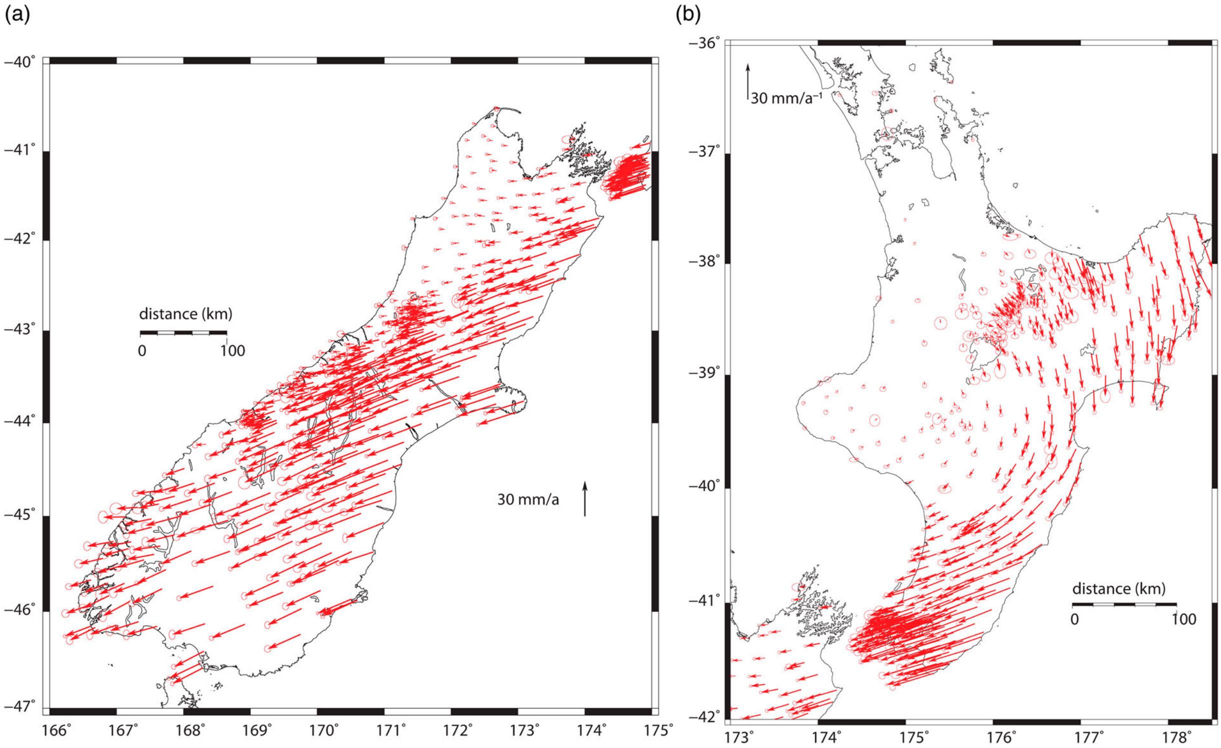

Figure 3. New Zealand GPS velocities in an Australian Plate fixed reference frame. **A**, South Island; **B**, North Island.

et al. 2010). The GPS sites in the southern South Island that underwent the largest displacements were also strongly affected by the 2003 Secretary Island earthquake. The offset from the Secretary Island earthquake that we determine at these sites in the Fiordland region (see preceding paragraph) will also include effects from the 2004 Macquarie Island earthquake, so we effectively correct for this at sites in the southern portion of the South Island in our offset calculation. However, due to lower level of displacement (≤5 mm) throughout the rest of New Zealand, we chose not to correct for the 2004 Macquarie Island earthquake elsewhere. Given the long duration of the New Zealand time series, the 2004 Macquarie Island earthquake will only affect the New Zealand campaign velocity estimates at the level of 0.25–0.05 mm a^{-1}.

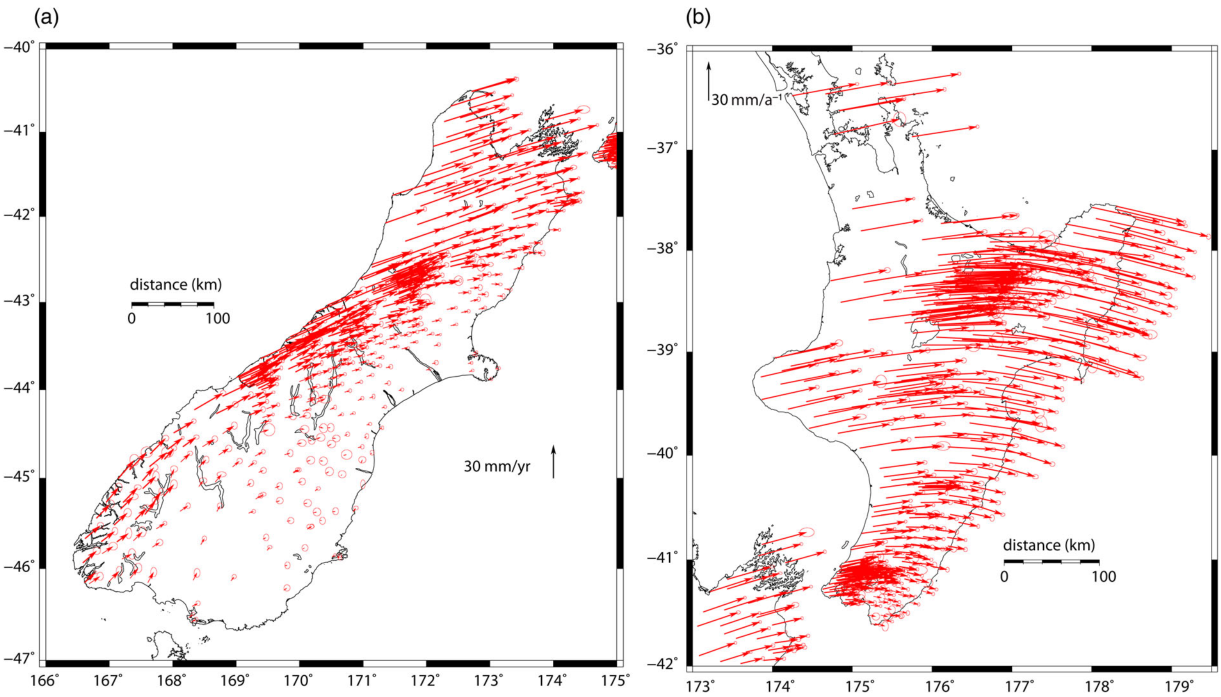

Figure 4. New Zealand GPS velocities in a Pacific Plate fixed reference frame. **A**, South Island; **B**, North Island.

Table 2. Table of earthquakes that have caused large displacements in the campaign network.

Date	Location/name	M_w
22 August 2003	Secretary Island, Fiordland	7.1
23 December 2004	Macquarie Island	8.1
15 October 2007	George Sound, Fiordland	6.7
15 July 2009	Dusky Sound	7.8
4 September 2010 (and subsequent aftershocks)	Darfield, Christchurch area	7.1

Assessment of velocity uncertainties

One of the most challenging aspects of GPS velocity field development is the calculation of reliable uncertainties. This is problematic, partly due to uncertainties in the appropriate noise models to use in these calculations (e.g. Williams et al. 2004; Shen et al. 2011; Dmitrieva et al. 2015). If the 'true' values of velocities at GPS sites are known, one test of reasonable velocity uncertainties is that the normalised residuals (e.g. the difference between the velocity estimate and the 'true' estimate multiplied by the uncertainties) should have a Gaussian distribution with zero mean and a variance of one. Although the 'true velocities' are impossible to know, particularly in complex deforming zones at plate boundaries, McCaffrey et al. (2007) and Shen et al. (2011) have addressed this by using predictions of the 'true velocities' at GPS sites in low-strain-rate areas using an elastic block model to calculate normalised residuals.

To evaluate the robustness of our uncertainty calculations, we undertake a similar analysis by calculating the predicted velocities at GPS sites in the low-strain-rate portions of the western North Island and northwestern South Island from an updated block model of Wallace et al. (2012a). Figure 5 shows the cumulative distribution of normalised residuals (e.g. the difference between the velocities predicted by the block model and those in Table S1, multiplied by the velocity uncertainties) compared to that predicted by the theoretical curve for a Gaussian distribution with variances of 1.0 (red) and 0.5 (green) for both the east and north components of the velocity residuals. Overall, the distribution of normalised residuals agrees reasonably well with the Gaussian curve with a variance of 1.0, although it fits the variance=0.5 curve even better. This suggests that we may have overestimated our uncertainties, perhaps by as much as 50%. Some users of this velocity field may therefore wish to scale our quoted uncertainties by 0.5, although to be conservative we prefer to use the values shown in Table S1.

Discussion and conclusions

With the exception of the earthquakes discussed under 'Outlier removal and coseismic deformation' above, no other major earthquakes have significantly impacted the campaign GPS network in New Zealand. We have largely removed or corrected for the influence of these earthquakes where possible, producing a velocity field that is representative of interseismic deformation in New Zealand during the 1995–2013 period (Figures 3, 4; Table S1).

The overall pattern of crustal motions observed in the new velocity field (Figure 3) is similar to that from previous New Zealand velocity fields (e.g. Beavan & Haines 2001; Wallace et al. 2012a). The major obvious features are a rapid clockwise rotation of the eastern North Island (e.g. Wallace et al. 2004) and strong shear associated with the Alpine Fault and Marlborough Fault System (e.g. Beavan & Haines 2001; Wallace et al. 2007). However, in addition to a longer duration of measurements, the new velocity field has much denser coverage in the Taupo Volcanic Zone (TVZ) and the Southland/Otago region than previously published velocity fields. In particular, the TVZ velocity field shows some surprising results. Sites west of the central TVZ are moving southeastwards at several millimetres per year relative to the Australian Plate, while many of the sites within the central TVZ have much lower rates of motion relative to the Australian Plate. This suggests strong contraction within the central TVZ (between Lake Taupo and Rotorua), which is at odds with the observation of active normal faulting within the central rift (e.g. Villamor & Berryman 2001). Holden et al. (2015) also observe such a contractional signal from their independent processing of data from the Okataina region. This contraction coincides with a large region of rapid subsidence (up to 2 cm a^{-1}) observed from interferometric synthetic aperture radar (InSAR) data, which Hamling et al. (2015) suggest is due to cooling of a magma body beneath the TVZ. It is likely that the observed GPS contraction is also related to magmatic cooling processes, and that it is masking tectonic deformation within the central TVZ (e.g. Holden et al. 2015).

Although we fit GPS velocities on the Australian Plate to within uncertainty (see Table S1, sites in Australia marked with **) with a single pole of rotation for the Australian Plate, many of the sites in the western portion of the North Island (Waikato and Northland regions; Figure 1) deviate from Australian Plate motion by as much as 0.5–3.0 mm a^{-1} (Figure 3B, Table S1), suggesting that the western North Island of New Zealand is not part of the stable Australian Plate. Tregoning et al. (2013) included a subset of the New Zealand continuous GPS sites in their processing of the global IGS network, and they showed that cGPS sites in the western North Island also deviate from Australian Plate motion. They estimated a pole of rotation for the western portion of the North Island, located near −36°S, 172°E, with a clockwise rotation rate of 0.28° Ma^{-1}. Our Australia-fixed velocity estimates at the same

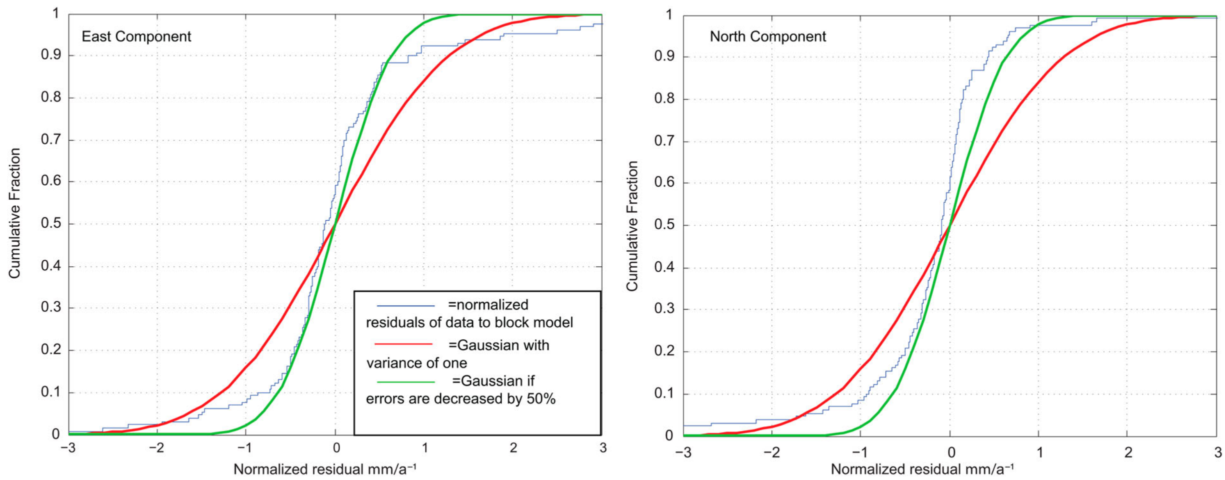

Figure 5. The distribution of normalised residuals (e.g. the difference between the velocities predicted by the block model of Wallace et al. 2012a and those in Table S1, normalised by their uncertainties) compared to that predicted by a theoretical curve for a Gaussian distribution with variances of 1.0 (red) and 0.5 (green), for both the east (left panel) and north (right panel) components of the velocity residuals.

cGPS sites (Table S1) agree with Tregoning et al.'s (2013) velocities to within uncertainty. Moreover, our velocities from those sites, and most of the campaign sites in Northland and Waikato, exhibit a similar, slow clockwise rotation about a pole offshore of the western North Island. This implies that much of the North Island is rotating in a similar fashion to that suggested for the Hikurangi forearc (e.g. Wallace et al. 2004; Figure 3B), albeit at a much slower rate (by a factor of c. 10). We also note that sites on the Coromandel Peninsula (CORM, A9MT; Figure 1) are moving eastwards relative to Auckland at 0.3–0.7 mm a^{-1}. This suggests that active faults which may exist within the Hauraki Gulf and onshore Hauraki Rift (such as the Kerepehi Fault) could be accommodating extension at rates on the order of 0.3–0.7 mm a^{-1}. Densification of campaign GPS networks in this region is needed to refine our understanding of this slowly deforming but potentially hazardous source of earthquakes for the highly populated Auckland region.

Likewise, all GPS sites on the east coast of the South Island exhibit c. 2–3 mm a^{-1} of northeastwards motion relative to the Pacific Plate (Figure 4), similar to that noted by Beavan et al. (2002). Some component of this northeastwards motion may be a result of elastic deformation from interseismic coupling on the Alpine Fault. The elastic block model of Wallace et al. (2007) predicts c. 1–2 mm a^{-1} of elastic deformation on the east coast of the South Island, due to locking on faults in the region. However, we cannot rule out the possibility that some low rates of deformation (<1–2 mm a^{-1}) also occur between the South Island and the Pacific Plate, accommodated along offshore structures east of New Zealand.

It is important to remember that there is strong temporal variability of deformation rates in parts of the North Island and northern South Island, particularly due to volcanic processes in the Taupo Volcanic Zone and the time-varying deformation on the Hikurangi subduction interface beneath the eastern North Island forearc and northern South Island during the period of campaign GPS measurements. However, these are not clearly discernible within the campaign GPS data and our velocities represent averages through these variations. The GeoNet continuous GPS network has revealed dozens of episodic slow slip events that have occurred on the Hikurangi subduction interface beneath the North Island (e.g. Wallace & Beavan 2010; Wallace et al. 2012b). The temporal resolution of the campaign velocity dataset is too low to correct for (or even identify) slow slip event behaviour in the North Island. The velocity field presented here is only intended to represent a snapshot of average deformation rates over the last c. 18 years, including deformation from slow slip events and interseismic coupling that occurred during that period. Analysis of the continuous GPS network data (www.geonet.org.nz), with its much higher temporal resolution, is necessary to investigate slow slip event and volcanic deformation, and any temporal variation in deformation rates over short timescales.

Supplementary data

Table S1. GPS velocities (in east component (V_E) and north components (V_N) in both ITRF2008 (IT08) and Australian Plate-fixed (AUS) reference frames, with uncertainties (σ_E and σ_N).

Acknowledgements

The co-authors of this paper are grateful to the late John Beavan for his major contributions to the development of a world-class geodetic dataset in New Zealand. This dataset has profoundly influenced our understanding of active plate boundary processes in New Zealand, and this legacy will undoubtedly live on. We also acknowledge the fundamental contributions of Desmond Darby, Graeme Blick and Chuck Meertens, who initiated the first GPS campaigns in New Zealand in the early 1990s. We also acknowledge the help of dozens of individuals in the field on GPS campaigns over the years; without their assistance the acquisition of this dataset would not have been possible. Insightful reviews by Duncan Agnew and one anonymous reviewer improved the quality of this paper.

Guest Editor: Dr Caroline Holden.

Disclosure statement

No potential conflict of interest was reported by the authors.

Funding

The acquisition of this dataset was made possible over many years by funding from a variety of sources, including the NZ Ministry for Science and Innovation (formerly the Foundation for Research, Science, and Technology); GNS Science; Land Information New Zealand; the New Zealand Earthquake Commission; University of Otago research grants; and various local and regional councils, including Greater Wellington. Some of the early campaign data (1996 and earlier) were acquired with funding obtained by overseas collaborators from science funding agencies in the United Kingdom and the United States.

References

Altamimi Z, Métivier L, Collilieux X. 2012. ITRF2008 plate motion model. J Geophys Res. 117:B07402. doi:10.1029/2011JB008930.

Beavan J. 2005. Noise properties of continuous GPS data from concrete pillar geodetic monuments in New Zealand and comparison with data from U.S. deep drilled braced monuments. J Geophys Res. 110:B08410. doi:10.1029/2005JB003642.

Beavan J, Ellis S, Wallace L, Denys P. 2007. Kinematic constraints from GPS on oblique convergence of the Pacific and Australian Plates, central South Island, New Zealand. In: Okaya D, Stern T, Davey F, editor. A continental plate boundary: tectonics at South Island, New Zealand. AGU Geophysical monograph series 175. doi:10.1029/175GM05.

Beavan J, Fielding E, Motagh M, Samsonov S, Donnelly N. 2011a. Fault location and slip distribution of the 22 February 2011 M_w 6.2 Christchurch, New Zealand, Earthquake from Geodetic data. Seismol Res Lett. 82:789–799.

Beavan J, Haines J. 2001. Contemporary horizontal velocity and strain-rate fields of the Pacific-Australian plate boundary zone through New Zealand. J Geophys Res. 106:741–770.

Beavan J, Moore M, Pearson C, Henderson M, Parsons B, Bourne S, England P, Walcott D, Blick G, Darby D, Hodgkinson K. 1999. Crustal deformation during 1994–1998 due to oblique continental collision in the central Southern Alps, New Zealand, and implications for seismic potential of the Alpine fault. J Geophys Res. 104:25233–25255.

Beavan J, Motagh M, Fielding E, Donnelly N, Collett D. 2012. Fault slip models of the 2010–2011 Canterbury, New Zealand, earthquakes from geodetic data and observations of postseismic ground deformation. New Zeal J Geol Geophys. 55:207–221.

Beavan J, Samsonov S, Denys P, Sutherland R, Palmer N, Denham M. 2011b. Oblique slip on the Puysegur subduction interface in the 2009 July M_w 7.8 Dusky Sound earthquake from GPS and InSAR observations: implications for the tectonics of southwestern New Zealand. Geophys J Int. 183:1265–1286.

Beavan J, Tregoning P, Bevis M, Kato T, Meertens C. 2002. Motion and rigidity of the Pacific Plate and implications for plate boundary deformation. J Geophys Res. 107:2261. doi:10.1029/2001JB000282.

Beavan J, Wallace L, Samsonov S, Ellis S, Motagh M, Palmer N. 2010. The Darfield (Canterbury) earthquake: geodetic observations and preliminary source model. Bull New Zeal Soc Earthq Eng. 43:228–235.

Bourne SJ, Arnadottir T, Beavan J, Darby D, England PC, Parsons B, Walcott RI, Wood PR. 1998. Crustal deformation of the Marlborough fault zone in the South Island of New Zealand: geodetic constraints over the interval 1982–1994. J Geophys Res. 103:30147–30165.

Dach R, Hugentobler U, Fridez P, Meindl M. 2007. Bernese GPS Software Version 5.0. Bern, Switzerland: Astronomical Institute, University of Bern. 612 p.

Darby D, Hodgkinson KM, Blick GH. 2000. Geodetic measurement of deformation in the Taupo Volcanic Zone, New Zealand: the North Taupo network revisited. New Zeal J Geol Geophys. 43:157–170.

Darby DJ, Beavan J. 2001. Evidence from GPS measurements for contemporary plate coupling on the southern Hikurangi subduction thrust and partitioning of strain in the upper plate. J Geophys Res. 106:30881–30891.

Darby DJ, Meertens CM. 1995. Terrestrial and GPS measurements of deformation across the Taupo backarc and Hikurangi forearc regions of New Zealand. J Geophys Res. 100:8221–8232.

DeMets C, Marquez-Azua B, Cabral-Cano E. 2014. A new GPS velocity field for the Pacific Plate—Part 1: constraints on plate motion, intraplate deformation, and the viscosity of Pacific basin asthenosphere. Geophys J Int. 199:1878–1899.

Denys P, Norris R, Pearson C, Denham M. 2014. A geodetic study of the Otago Fault System of the South Island of New Zealand. In: Rizos C, Willis P, editor. Earth on the edge: science for a sustainable planet. International Association of Geodesy Symposia 139. Berlin: Springer; p. 151–158. doi:10.1007/978-3-642-37222-3_19.

Dmitrieva K, Segall P, DeMets C. 2015. Network-based estimation of time-dependent noise in GPS position time-series. J Geodesy. 89:591–606.

Elliott J, Freymueller JT, Larsen CF. 2013. Active tectonics of the St. Elias orogen, Alaska, observed with GPS measurements. J Geophys Res Solid Ear. 118:5625–5642. doi:10.1002/jgrb.50341.

Ellis S, Beavan J, Eberhart-Phillips D, Stöckhert B. 2006b. Simplified models of the Alpine Fault seismic cycle: Stress transfer in the mid-crust. Geophys J Int. doi:10.1111/j.1365-246X. 2006.02917.x.

Ellis S, Beavan J, Eberhart-Phillips D. 2006a. Bounds on the width of mantle lithosphere flow derived from surface geodetic measurements: application to the central Southern Alps, New Zealand. Geophys J Int. doi:10.1111/j.1365-246X.2006.02918.x.

Gledhill K, Ristau J, Reyners M, Fry B, Holden C. 2011. The Darfield (Canterbury, New Zealand) M_w 7.1 Earthquake

of September 2010: a preliminary seismological report. Seismol Res Lett. 82:378–386.
Hamling IJ, Hreinsdóttir S, Fournier N. 2015. The ups and downs of the TVZ: geodetic observations of deformation around the Taupo Volcanic Zone, New Zealand. J Geophys Res. 120:4667–4679. doi:10.1002/2015JB012125.
Herring T, King RW, McClusky, SC. 2010. GLOBK reference manual, version 10.4. Cambridge: Massachusetts Institute of Technology.
Holden L, Wallace L, Beavan J, Fournier N, Cas R, Ailleres L, Silcock D. 2015. Contemporary ground deformation in the Taupo Rift and Okataina Volcanic Centre from 1998–2011, measured using GPS. Geophys J Int. 202:2082–2105.
Langbein J. 2012. Estimating rate uncertainty with maximum likelihood: differences between power-law and flicker-random walk models. J Geodesy. 86:775–783.
Mazzotti S, Leonard LJ, Cassidy JF, Rogers GC, Halchuk S. 2011. Seismic hazard in western Canada from GPS strain rates versus earthquake catalog. J Geophys Res. 116. doi:10.1029/2011JB008213.
McCaffrey R, Qamar AI, King RW, Wells R, Khazaradze G, Williams CA, Stevens CW, Volick JJ, Zwick PW. 2007. Fault locking, block rotation and crustal deformation in the Pacific Northwest. Geophys J Int. 169:1315–1340.
Moore M, England P, Parsons B. 2002. Relation between surface velocity field and shear wave splitting in the South Island of New Zealand. J Geophys Res. 107:2198. doi:10.1029/2000JB000093.
Nicol A, Beavan J. 2003. Shortening of an overriding plate and its implications for slip on a subduction thrust, central Hikurangi Margin, New Zealand. Tectonics. 22. doi:10.1029/2003TC001521.
Nicol A, Wallace LM. 2007. Temporal stability of deformation rates: comparison of geological and geodetic observations, Hikurangi subduction margin, New Zealand. Earth Planet Sc Lett. doi:10.1016/j.epsl.2007.03.039.
Niell AE. 1996. Global Mapping Functions for the Atmospheric Delay at Radio Wavelengths. J Geophys Res. 101:3227–3246.
Petersen T, Ristau J, Beavan J, Denys P, Denham M, Field B, Francois-Holden C, McCaffrey R, Palmer N, Reyners M, Samsonov S, GeoNet team. 2009. The M_w 6.7 George Sound earthquake of October 15, 2007: response and preliminary results. Bull New Zeal Soc Earthq Eng. 42:129–141.
Reilinger R, McClusky S, Vernant P, Lawrence S, Ergintav S, Cakmak R, Ozener H, Kadirov F, Guliev I, Stepanyan R, et al. 2006. GPS constraints on continental deformation in the Africa-Arabia-Eurasia continental collision zone and implications for the dynamics of plate interactions. J Geophys Res. 111:B05411.
Reyners M, McGinty P, Cox S, Turnbull I, O'Neill T, Gledhill KR, Hancox G, Beavan J, Matheson D, Mcverry G, et al. 2003. The M_w 7.2 Fiordland earthquake of August 21, 2003: background and preliminary results. Bull New Zeal Soc Earthq Eng. 36:233–248.
Shen Z-K, King RW, Agnew DC, Wang M, Herring TA, Dong D, Fang P. 2011. A unified analysis of crustal motion in Southern California, 1970–2004: the SCEC crustal motion map. J Geophys Res. 116:B11402.
Stirling M, McVerry G, Gerstenberger M, Litchfield N, Van Dissen R, Berryman K, Barnes P, Wallace L, Villamor P, Langridge R, et al. 2012. National seismic hazard model for New Zealand: 2010 update. B Seismol Soc Am. 102:1514–1542.
Tregoning P, Burgette R, McClusky SC, Lejeune S, Watson CS, McQueen H. 2013. A decade of horizontal deformation from great earthquakes. J Geophys Res: Solid Earth. 118:2371–2381. doi:10.1002/jgrb.50154.
Villamor P, Berryman K. 2001. A late Quaternary extension rate in the Taupo Volcanic Zone, New Zealand, derived from fault slip data. New Zeal J Geol Geophys. 44:243–269.
Wallace LM, Barnes P, Beavan RJ, Van Dissen RJ, Litchfield NJ, Mountjoy J, Langridge RM, Lamarche G, Pondard N. 2012a. The kinematics of a transition from subduction to strike-slip: an example from the central New Zealand plate boundary. J Geophys Res Solid Eart. doi:10.1029/2011JB008640.
Wallace LM, Beavan J. 2010. Diverse slow slip behavior at the Hikurangi subduction margin, New Zealand. J Geophys Res. 115. doi:10.1029/2010JB007717.
Wallace LM, Beavan J, Bannister S, Williams CA. 2012b. Simultaneous long- and short-term slow slip events at the Hikurangi subduction margin, New Zealand: implications for processes that control slow slip event occurrence, duration, and migration. J Geophys Res. doi:10.1029/2012JB009489.
Wallace LM, Beavan J, McCaffrey R, Darby D. 2004. Subduction zone coupling and tectonic block rotation in the North Island, New Zealand. J Geophys Res. 109. doi:10.1029/2004JB003241.
Wallace LM, Beavan RJ, McCaffrey R, Berryman KR, Denys P. 2007. Balancing the plate motion budget in the South Island, New Zealand using GPS, geological and seismological data. Geophys J Int. 168. doi:10.1111/j.1365-246X.2006.03183.x.
Watson C, Burgette R, Tregoning P, White N, Hunter J, Coleman R, Handsworth R, Brolsma H. 2010. Twentieth century constraints on sea level change and earthquake deformation at Macquarie Island. Geophys J Int. 182:781–796.
Williams SDP, Bock Y, Fang P, Jamason P, Nikolaidis RM, Prawirodirdjo L, Miller M, Johnson DJ. 2004. Error analysis of continuous GPS position time series. J Geophys Res. 109. doi:10.1029/2003JB002741.
Zhang J, Bock Y, Johnson H, Fang P, Williams S, Genrich J, Wdowinski S, Behr J. 1997. Southern California permanent GPS geodetic array: Error analysis of daily position estimates and site velocities. J Geophys Res. 102:18035–18055.
Zhang P-Z, Shen Z, Wang M, Gan W, Burgmann R, Molnar P, Wang Q, Niu Z, Sun J, Wu J, Hanrong S, Xinzhao Y. 2004. Continuous deformation of the Tibetan Plateau from global positioning system data. Geology. 32:809–12.